Conductance Fluctuations in Mesoscopic Normal-Metal/Superconductor Samples

Klaus Hecker,[1] Helmut Hegger,[1] Alexander Altland,[2,3] and Klaus Fiegle[4]
[1]*Physikalisches Institut, Universität zu Köln, D-50937 Köln, Germany*
[2]*Institut für Theoretische Physik, Universität zu Köln, D-50937 Köln, Germany*
[3]*Cavendish Laboratory, Madingley Road, Cambridge CB3 0HE, United Kingdom*
[4]*I. Physikalisches Institut, Universität zu Köln, D-50937 Köln, Germany*
(Received 10 February 1997)

We study the magnetoconductance fluctuations of mesoscopic normal-metal/superconductor (NS) samples consisting of a gold wire in contact with a niobium film. The magnetic field strength is varied over a wide range, including values that are larger than the upper critical field B_{c2} of niobium. In agreement with recent theoretical predictions we find that in the NS sample the rms of the conductance fluctuations (CF) is by a factor of 2.8 ± 0.4 larger than in the high field regime where the entire system is driven normal conducting. Further characteristics of the CF are discussed. [S0031-9007 (97)03879-9]

PACS numbers: 73.23.–b, 73.50.Jt, 74.80.–g

At low temperatures disordered metals smaller than the phase coherence length L_φ (mesoscopic systems) exhibit a host of quantum fluctuation phenomena like, e.g., universal fluctuations of the electrical conductance [1–3]. Recently it has become clear that additional mechanisms of quantum coherence arise when a mesoscopic normal metal sample (N) is brought in contact with a superconductor (S) [4,5,6–16]. These processes, which are caused by the interference of electrons and Andreev reflected holes [17], manifest themselves in the emergence of additional universality classes [4] and an altered fluctuation behavior of various mesoscopic observables. In particular the fluctuations of the magnetoconductance are still universal of order e^2/h but tend to exceed the normal-metal fluctuations by numerical factors of order unity. These enhancement factors are a consequence of (i) the fact that *two* elementary charges are transferred per Andreev reflection [4,5,12,13] and (ii) the presence of diffusionlike modes which are absent in the pure N-case. To be specific, it has been found that in the presence of an external magnetic field the rms amplitude of the conductance fluctuations $\mathrm{rms}(G_{\mathrm{NS}})$ exceeds its normal metal $\mathrm{rms}(G_{\mathrm{N}})$ value by a factor of $2\sqrt{2}$. This result holds true in the presence [4] or absence [4,5] of spin-orbit scattering.

The fluctuation characteristics of a NS sample are strongly affected by magnetic fields. At least three different regimes with qualitatively different behavior can be identified [cf. Fig.1(a)]: (i) The presence of the proximity effect gives rise to a resistance minimum for small magnetic fields. In our samples the proximity effect is suppressed by fields of order $B_1 \sim 0.1$ T [18]. (ii) For intermediate fields larger than B_1 but smaller than the upper critical field of the superconductor B_{c2}, the proximity effect is suppressed, but the process of Andreev reflection is still active. (iii) For fields larger than B_{c2} the superconductivity is globally destroyed.

Most experiments of other groups were performed in regime (i) [7–11]. In contrast, we have studied the magneto-CF in the regimes (ii) and (iii). We are thus in a position to compare the fluctuation behavior of *one and the same sample* in both regimes NS and pure N. As a result, we find that the CF of the NS system are enhanced as compared to those of the N system. The ratio $\mathrm{rms}(G_{\mathrm{NS}})/\mathrm{rms}(G_{\mathrm{N}})$ turns out to be in good agreement with the theoretical prediction.

The inset of Fig. 1(a) shows the sample layout. The sample consists of a Nb contact, a mesoscopic Au wire, and a second Au contact. This layout corresponds to a mesoscopic two-probe arrangement [19]. Far outside the coherence volume the two contacts are split-up to perform a macroscopic four-point measurement. The samples were prepared in two successive steps using electron-beam lithography and lift-off technique [20]. In a first step the Nb contact was prepared by *in situ* deposition of a 30 nm Nb and a 10 nm Au layer, which prevents oxidation of the Nb. In a second process the Au wire of length $L \simeq 1\ \mu$m (width $W \simeq 180$ nm, thickness $t \simeq 30$ nm) and the Au contact was produced. Both the Nb and Au layers were dc magnetron sputtered. We report on measurements of two samples which had a normal state resistance $R_{\mathrm{N}} \sim 15\ \Omega$ at low temperatures (see Table I). From the residual resistance ratio and from the sheet resistance of wide Nb and Au films of the same thickness we derive elastic mean free paths of $\ell_{\mathrm{Au}} \simeq 32$ nm, $\ell_{\mathrm{Nb}} \simeq 5$ nm, and diffusion constants of $D_{\mathrm{Au}} \simeq 150\ \mathrm{cm}^2/s$, $D_{\mathrm{Nb}} \simeq 23\ \mathrm{cm}^2/s$. The Thouless energy $E_{\mathrm{Th}} = hD_{\mathrm{Au}}/L_\varphi^2$ for our systems is $E_{\mathrm{Th}} \simeq 100\ \mu$eV [21]. The critical temperature of the Nb is $T_c \simeq 8$ K, for Nb films with and without a Au layer, and $B_{c2}(T = 100\ \mathrm{mK}) \simeq 2.5$ T. The measurements were performed in a ^{3}He-^{4}He dilution refrigerator at temperatures down to $T_{\mathrm{min}} \simeq 45$ mK [19]. The conductance $G(B)$ was measured by means of a standard lock-in technique for magnetic fields up to $B = 9$ T. We used small measurement currents $I_{\mathrm{ac}} = 1$–$3\ \mu$A at temperatures below 1 K. Larger currents were used at $T > 1$ K always under the condition $V_{\mathrm{ac}} < k_B T/e$.

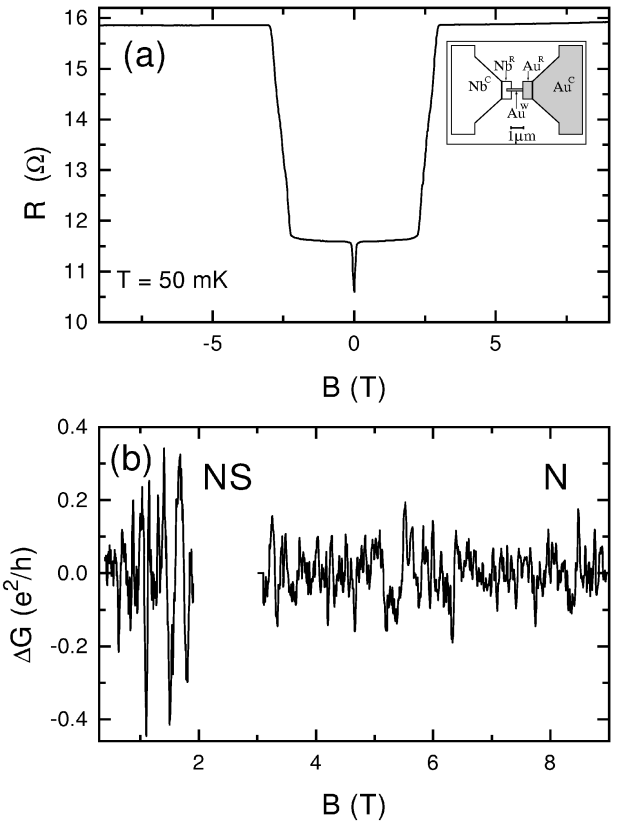

FIG. 1. (a) Magnetoresistance of sample 1. Three regimes can be identified: (i) For small magnetic fields ($B_1 \simeq 0.1$ T) a proximity effect induced resistance minimum is observed. (ii) In the field range $B \simeq 0.4-2$ T the resistance is approximately constant. (iii) For $B > 3.1$ T the whole sample is driven normal conducting. The inset shows the sample geometry: A mesoscopic Au wire (Au^W, length $L \simeq 1$ μm, width $W \simeq$ 180 nm) is connected to a Nb contact ($Nb^C + Nb^R$) and an Au contact ($Au^R + Au^C$) (mesoscopic two-probe arrangement). (b) Conductance fluctuations of sample 1 in the NS-case ($0.4 < B < 1.9$ T) $\mathrm{rms}(G_{\mathrm{NS}}) = (0.16 \pm 0.02)e^2/h$ and the N-case ($3.1 < B < 9$ T) $\mathrm{rms}(G_{\mathrm{N}}) = (0.058 \pm 0.003)e^2/h$.

We now turn to the discussion of our results. Figure 1(b) shows the conductance fluctuations for both the NS and the N-case as a function of the magnetic field. Since the magnetoconductance is measured in a mesoscopic two-probe configuration, its fluctuations are symmetric with respect to a reversal of the magnetic field [19,22]. For this reason, only the part $B > 0$ T of the magnetofingerprints $\Delta G(B)$ is shown. The NS-CF at low magnetic fields are clearly larger than in the N-case ($B \geq 3.1$ T).

We obtain values of $\mathrm{rms}(G_{\mathrm{NS1}}) = 0.16 \pm 0.02\ e^2/h$ and $\mathrm{rms}(G_{\mathrm{N1}}) = (0.058 \pm 0.003)e^2/h$ for sample 1 (see Table I and Figs. 1–3). For sample 2 the rms values are slightly smaller: $\mathrm{rms}(G_{\mathrm{NS2}}) = 0.14 \pm 0.02\ e^2/h$ and $\mathrm{rms}(G_{\mathrm{N2}}) = (0.050 \pm 0.004)e^2/h$ (see Table I and Fig. 3). Since the magnetic-field range for the calculation of the NS-CF is much smaller ($\Delta B_{\mathrm{NS}} = 1.5$ T) than the range of the N-CF ($\Delta B_{\mathrm{N}} = 5.9$ T) the uncertainty for the $\mathrm{rms}(G_{\mathrm{NS}})$ values is substantially larger.

We note that the measured values of the CF are much smaller than the results obtained in zero temperature theoretical calculations. To understand better the origin of this discrepancy, viz. the combined effect of finite temperatures and dephasing effects, let us briefly recall a few known theoretical predictions about the CF of diffusive mesoscopic systems. As has been shown diagrammatically (cf. [2], and references therein) the CF of quasi-one-dimensional wires in the presence of both spin-orbit interactions and a magnetic field are given by

$$\left.\begin{matrix}\mathrm{rms}(G_{\mathrm{N}})^2 \\ \mathrm{rms}(G_{\mathrm{NS}})^2\end{matrix}\right\} = \frac{6e^4}{h^2}\left\langle \sum_q \left(\frac{hD/L_{\mathrm{eff}}^2}{hDq^2 + h/\tau_\varphi + i\epsilon} \right)^2 \right\rangle_\epsilon \times \begin{cases} 1 \\ 8 \end{cases}. \quad (1)$$

Here $\langle \cdots \rangle_\epsilon := \frac{1}{2k_BT} \int_{-k_BT}^{k_BT} d\epsilon (\cdots)$ stands for a temperature induced energy averaging procedure [2], $\sum_q$ denotes a summation over quantized momenta $q = \pi/L_{\mathrm{eff}}$, $2\pi/L_{\mathrm{eff}}, \ldots$ and it has been assumed that the wire's cross section $L_\perp \ll L_{\mathrm{eff}}$ (i.e., $hD/L_\perp^2$ is by far larger than any relevant energy scale in the problem, which means that the wire can be regarded as "quasi"-one-dimensional [2]).

TABLE I. R_{N}: Normal state resistance at $T = 50$ mK and $B = 4$ T, R_{NS}: Resistance in the intermediate regime (ii) at $T = 50$ mK and $B = 1$ T (see Fig. 1).

	Sample 1	Sample 2
R_{N} (Ω)	15.87	14.34
R_{NS} (Ω)	11.60	9.72
$\mathrm{rms}(G_{\mathrm{NS}})$ (e^2/h)	0.16 ± 0.02	0.14 ± 0.02
$\mathrm{rms}(G_{\mathrm{N}})$ (e^2/h)	0.058 ± 0.003	0.050 ± 0.004
$\mathrm{rms}(G_{\mathrm{NS}})/\mathrm{rms}(G_{\mathrm{N}})$	2.8 ± 0.4	2.8 ± 0.4

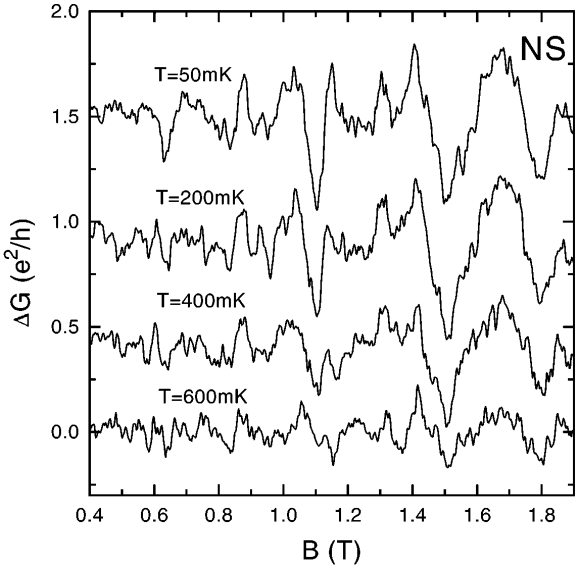

FIG. 2. NS conductance fluctuations of sample 1 for different temperatures. For temperatures $T \geq 300$ mK the CF are reduced (cf. Fig. 3). Traces are shifted for clarity.

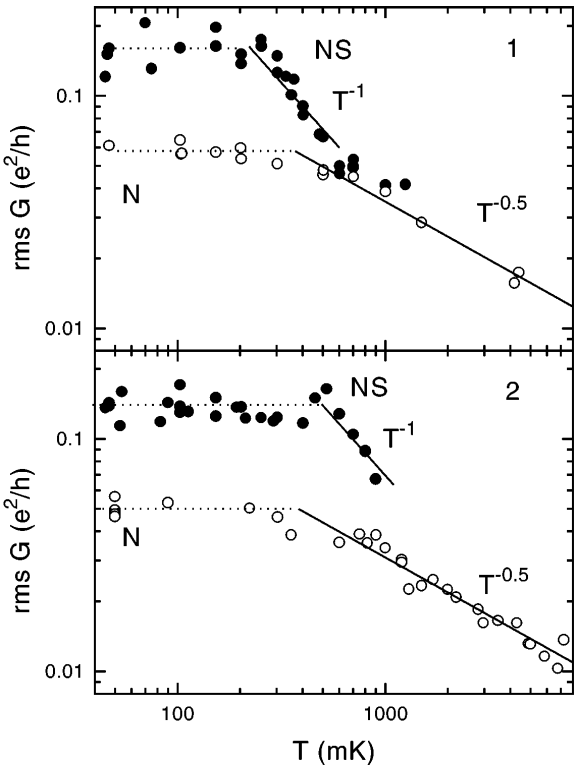

FIG. 3. rms amplitudes of the NS-CF (●) and the N-CF (○) for sample 1 (upper panel) and sample 2 (lower panel). The dotted lines show the low temperature saturation values (cf. Table I). The reduction of rms$[G_{\rm NS}(T)]$ starts at about 300–500 mK. The N-CF sets are reduced for $T \geq 400$ mK. The solid lines correspond to T^{-1} (NS) and $T^{-0.5}$ (N) power laws.

The phenomenological parameter τ_φ ($L_\varphi = \sqrt{D\tau_\varphi}$) accounts for the various dephasing mechanisms which lead to a destruction of the conductance fluctuations. Whereas the formula for the N-case can be found at various places in the literature (cf., e.g., [23] for a reference with correct prefactors) the NS formula is less standard and deserves a few comments. The relative factor of 8 results from (a) the fact that two elementary charges are driven through the system whenever an Andreev reflection occurs ($e \rightarrow 2e$) and (b) the presence of twice as many diffusionlike modes as in the N regime. These additional modes are in many respects similar to the standard diffusive modes (cf. the discussion in Ref. [4]), that is their presence manifests in an additional factor of 2 (rather than in a structurally altered formula). We emphasize that in a normal metal, the scale $L_{\rm eff}$ appearing in (1) represents the *effective* length of the sample, i.e., the length of the region where most of the voltage drops. In a NS sample, however, $L_{\rm eff}$ is *twice* that length. This is a consequence of the fact that both the incoming electrons and the outgoing holes have to traverse the system diffusively [5,12].

We next discuss the absolute magnitude of the CF. Equation (1) contains most of the information about conductance fluctuations we need to know. In the limit of low temperatures and vanishing inelastic interactions ($T, \tau_\varphi^{-1} \rightarrow 0$), Eq. (1) yields the universal values $\mathrm{rms}(G_{\rm N}^{\rm theo}) = 0.258\ e^2/h$ and $\mathrm{rms}(G_{\rm NS}^{\rm theo}) = 0.729\ e^2/h$. In our experiment, however, the low temperature regime is characterized by the inequality $L_T > L_{\rm eff} \gg L_\varphi$, where $L_\varphi = (D\tau_\varphi)^{1/2}$ and $L_T = (hD/k_BT)^{1/2}$ are the dephasing and thermal length, respectively. Under these circumstances the conductance fluctuations are reduced by a factor $\sim(L_\varphi/L_{\rm eff})^{(4-d)/2}$ below their universal, length independent value (d: dimensionality of the system). In order to interpret the experimental data we therefore carefully have to estimate the scale $L_{\rm eff}$, i.e., the size of the sample region that contributes most to the resistance (or equivalently to the conductance fluctuations).

It is evident from the sample geometry shown in the inset of Fig. 1(a), that the main part of the voltage drop occurs in the narrow wire $\mathrm{Au^W}$. The resistance of the wide contacts [$\mathrm{Nb^C} + \mathrm{Nb^R}$ and $\mathrm{Au^R} + \mathrm{Au^C}$ in Fig. 1(a)] is about $1.2R_\square$ each ($R_\square$: sheet resistance). The main voltage drop of a contact is located at the small rectangles $\mathrm{Nb^R}$ and $\mathrm{Au^R}$ corresponding to a resistance of about $0.5R_\square$. The sheet resistances of the Nb and the Au differ by a factor of about 4 ($R_\square^{\rm Nb} \simeq 4\ \Omega$, $R_\square^{\rm Au} \simeq 0.9\ \Omega$). Thus the contribution of the Au rectangle $\mathrm{Au^R}$ is about 0.5 Ω, which is less than 5% of the total resistance and neglected in the following. Hence, in the NS-case the voltage drop can be attributed to the wire $\mathrm{Au^W}$. We obtain an effective length of $L_{\rm eff}^{\rm NS} \simeq 2L \simeq 2\ \mu$m. In the case where the whole sample is normal conducting the situation is different. The Nb rectangle $\mathrm{Nb^R}$ has a resistance of about 2 Ω corresponding to 13% of the total resistance. The region contributing to the voltage drop is thus larger in the N-case. Here, $L_{\rm eff}$ is given by the regions $\mathrm{Au^W}$ *and* $\mathrm{Nb^R}$ resulting in $L_{\rm eff}^{\rm N} \simeq 1.8\ \mu$m. Of course, this is only a rough estimate for the effective lengths of the samples. The main conclusion to be drawn is that the effective lengths $L_{\rm eff}$ are *roughly the same in both the N-case and the NS-case*. To check the validity of the above consideration we have calculated the phase coherence length of the system via $L_\varphi = L_{\rm eff}[\mathrm{rms}\,(G_{\rm exp})/\mathrm{rms}(G_{\rm theo})]^{2/3}$ using the previously estimated values of $L_{\rm eff}$. The dephasing length L_φ is expected to be roughly independent of the strength of the magnetic field (as long as the latter is sufficiently strong to break time reversal invariance). Indeed we obtain almost constant values $L_\varphi \simeq 660 \pm 60$ nm for the different regimes and samples [24], thereby supporting the correctness of our estimates for $L_{\rm eff}$. Furthermore, the value for L_φ is in good agreement with previous studies [19,22].

Since $L_{\rm eff}^{\rm NS} \simeq L_{\rm eff}^{\rm N}$, we can directly compare the respective rms values of the CF. We obtain a ratio of

$$\frac{\mathrm{rms}(G_{\rm NS})}{\mathrm{rms}(G_{\rm N})} = 2.8 \pm 0.4 \qquad (2)$$

for both samples (see Table I). This ratio is in agreement with the theoretical value of $2\sqrt{2}$ [4,5]. Earlier theoretical work predicted an enhancement by only a factor of 2 [12].

In contrast, the experiment confirms the recent results of Altland and Zirnbauer [4] and Brouwer and Beenakker [5]. Equation (2) represents the central result of our experiment. In the next few paragraphs we report on further characteristics of the NS fluctuations, in particular on their temperature and voltage dependence.

Figure 2 shows NS magnetofingerprints in the temperature range between 50 and 600 mK. Up to $T \simeq 300$ mK we observe the low temperature saturation value of $\mathrm{rms}(G_{\mathrm{NS}}) = 0.16 \pm 0.02\ e^2/h$, as shown in Fig. 3. For higher temperatures the CF are suppressed and follow a $T^{-1\pm0.1}$ law. A similar behavior is observed for sample 2 (cf. Fig. 3). Here the reduction starts at a somewhat higher temperature $T \simeq 400$ mK. The N-CF were investigated for temperatures between 45 mK and 7 K (cf. Fig. 3). The reduction of the N-CF starts at $T \geq 400$ mK and follows a $T^{-0.50\pm0.05}$ law for both samples.

In general, CF are suppressed as soon as either $L_\varphi(T)$ or L_T become smaller than L_{eff} [cf. Eq. (1)]. For higher temperatures they show a weak power law behavior [2] $\mathrm{rms}[G(T)] \sim T^{-\alpha}$. The exponent depends on various system characteristics such as the ratio between the different length scales, and its dimensionality. However, we do not have a compelling argument for why α should depend on the presence or absence of superconductivity. In other words, a conclusive explanation of the different power-law behaviors observed in the experiment is lacking. Nevertheless, we would like to speculate on a mechanism that *might* be responsible for this effect: We observe that the rms amplitudes of the NS-CF and the N-CF saturate at low temperatures although $L_{\mathrm{eff}} > L_\varphi$ in our samples. We therefore conclude that L_φ must be almost temperature independent at low temperatures. If the temperature is raised, L_T and L_φ decrease and thereby the CF. The point now is that the decay rate of the CF sensitively depends on the effective dimensionality of the sample—the lower the dimensionality, the higher the decay rate (cf. Ref. [2] for details). In regime (ii) our systems are clearly quasi-one-dimensional. However, in (iii) the situation is different since the effectively two-dimensional wide Nb electrode contributes to the CF. This might give rise to a less pronounced temperature dependence. Nonetheless, it seems to be unlikely that a dimensional crossover of this kind can account for the whole effect.

Let us finally comment on the dependence of the CF on the measuring voltage. Voltages V exceeding the value $V_{\mathrm{Th}} = E_{\mathrm{Th}}/e$ break the symmetry between particles and holes, thereby leading to a destruction of the above mentioned additional diffusive modes. In our samples $V_{\mathrm{Th}} \simeq 100\ \mu$V [4,5,13,14]. Indeed, we do not observe any influence of V_{ac} on size or temperature dependence of the NS-CF up to $V_{\mathrm{ac}} = 35\ \mu$V, which is of the same order as V_{Th}. For higher voltages $\mathrm{rms}(G_{\mathrm{NS}})$ is reduced.

To summarize, we have measured the magnetoconductance fluctuations of mesoscopic Au/Nb systems. By changing the magnetic field strength we induced a crossover from a normal-superconducting to a purely normal-conducting state. We found a relative enhancement factor $\mathrm{rms}(G_{\mathrm{NS}})/\mathrm{rms}(G_{\mathrm{N}}) = 2.8 \pm 0.4$ in good agreement with the theoretical prediction $\mathrm{rms}(G_{\mathrm{NS}}^{\mathrm{theo}})/\mathrm{rms}(G_{\mathrm{N}}^{\mathrm{theo}}) = 2\sqrt{2}$ [4]. For large temperatures the NS-CF behave like $\mathrm{rms}[G_{\mathrm{NS}}(T)] \sim 1/T$, thereby showing a stronger temperature dependence than the N-CF.

We thank R. Gross, K. Jacobs, D. E. Khmelnitskii, H. Micklitz, A. Nowack, and M. Zirnbauer for useful discussions. This work was supported by the Deutsche Forschungsgemeinschaft through SFB 341 and SFB 301 and by BMBF, Grants No. 052KV134-(6) and No. 053KU234-(0).

[1] P. A. Lee and A. D. Stone, Phys. Rev. Lett. **55**, 1622 (1985); B. L. Al'tshuler, Sov. Phys. JETP Lett. **12**, 648 (1985).
[2] P. A. Lee, A. D. Stone, and H. Fukuyama, Phys. Rev. B **35**, 1039 (1987).
[3] S. Washburn and R. A. Webb, Rep. Prog. Phys. **55**, 1311 (1992), and references therein.
[4] A. Altland and M. R. Zirnbauer, Phys. Rev. B **55**, 1142 (1997).
[5] P. W. Brouwer and C. W. J. Beenakker, Phys. Rev. B **52**, 16 772 (1995).
[6] A. Kastalsky *et al.*, Phys. Rev. Lett. **67**, 3026 (1991).
[7] V. T. Petrashov *et al.*, Phys. Rev. Lett. **74**, 5268 (1995).
[8] S. G. den Hartog *et al.*, Phys. Rev. Lett. **76**, 4592 (1996); S. G. den Hartog *et al.*, Phys. Rev. Lett. **77**, 4954 (1996).
[9] H. Courtois *et al.*, Phys. Rev. Lett. **76**, 130 (1996).
[10] S. Guéron *et al.*, Phys. Rev. Lett. **77**, 3025 (1996).
[11] P. Charlat *et al.*, Phys. Rev. Lett. **77**, 4950 (1996).
[12] Y. Takane and H. Ebisawa, J. Phys. Soc. Jpn. **61**, 2858 (1992).
[13] I. K. Marmorkos, C. W. J. Beenakker, and R. A. Jalabert, Phys. Rev. B **48**, 2811 (1993).
[14] P. W. Brouwer and C. W. J. Beenakker, Phys. Rev. B **52**, R3868 (1995).
[15] Y. V. Nazarov and T. H. Stoof, Phys. Rev. Lett. **76**, 823 (1996).
[16] A. F. Volkov, N. Allsopp, and C. J. Lambert, J. Phys. Condens. Matter **8**, L45 (1996).
[17] A. F. Andreev, Sov. Phys. JETP **19**, 1228 (1964).
[18] In zero magnetic field a reentrance of metallic conductivity occurs at low temperatures and voltages [11]. We observe a resistance minimum at $T \simeq 1$ K in $R(T)$ and at $V_{\mathrm{dc}} \simeq 100\ \mu$V in *IV* characteristics.
[19] K. Hecker *et al.*, Phys. Rev. B **50**, 18 601 (1994).
[20] K. Fiegle, D. Diehl, and K. Jacobs, IEEE Trans. Appl. Supercond. **7**, 3552 (1997).
[21] D. J. Thouless, Phys. Rev. Lett. **39**, 1167 (1977).
[22] H. Hegger *et al.*, Phys. Rev. Lett. **77**, 3885 (1996).
[23] B. L. Altshuler, V. Kravtsov, and I. V. Lerner, Sov. Phys. JETP **64**, 1352 (1986).
[24] As we do not observe a weak-localization contribution to the conductance the exact value of L_φ cannot be evaluated in our samples.